UDC621.771.26:681.3:519.6

Analysis of Long Steel Product Rolling by Rigid-Plastic Finite Element Method

Kazunori Seki*1 Kenji Yamada*1
Shinji Ida*1 Shuichi Hamauzu*1
Shin-ya Hayashi*1 Matsuo Ataka*1

Abstract:

A three-dimensional steady-state rigid-plastic finite element method code and a preprocessing code for preparing a rational streamline profile as the initial analytical conditions were developed. Using these codes, a general-purpose system was developed for analyzing the rolling of long steel products, such as bars, wire and rod, shapes, and rails. This analytical system can adapt to any material cross-sectional shape, roll groove geometry, or roll arrangement. It can also simulate processes for rolling almost any type of long steel product. Hollow blooms, angles, and H shapes were analyzed as the application examples of the system.

1. Introduction

The rolling of long steel products, such as bars, wire and rod, shapes, and rails, involves three-dimensional deformation, uses various types of roll grooves and mills, and is difficult to handle theoretically. The experience of skilled engineers has played an important role in the design of these long steel product rolling processes. Researchers have made attempts, mainly experimental, to clarify the rolling characteristics of long steel products, but found it difficult to obtain a wide range of systematic information.

The increasing capacity and speed of computers in recent years have enabled the analysis of long steel product rolling by the three-dimensional rigid-plastic finite element method (FEM)[1-4], the study of the deformation and loading characteristics of bars[5] and angles[6], and the construction of an expert system for the breakdown process of H shapes from a database of FEM analytical results[7]. The present authors developed a three-dimensional rigid-plastic FEM code and used it to analyze mandrel rolling[8] and H-shape universal rolling[9].

For efficient analysis of long steel product rolling, the analytical technique employed must be versatile as well as accurate. A general-purpose preprocessing code was created and combined with the three-dimensional rigid-plastic FEM code already reported[9] to build a general-purpose long-steel product rolling analytical system. This paper gives an overview of the analytical system and presents analytical examples of hollow bloom rolling, rough rolling of angles, and web width increase rolling of H shapes.

*1 Technical Development Bureau

2. Long Steel Product Rolling Analytical System

2.1 Description of analytical system

The flow of rolling analysis by the system is shown in **Fig. 1**. The input data are the cross-sectional shape of the material before rolling and the groove shape and arrangement of the rolls. They are entered as parameters. In the preprocessing stage, the initial streamline profile (mesh) and boundary conditions required for the analysis are automatically calculated. In the deformation analysis stage, the velocity field is analyzed by a method based on the theory of plasticity for slightly compressible solids[10], the streamline profile is then corrected on the basis of contact analysis, and the node velocity, strain, stress and the like are computed. The analytical results are displayed by a general preprocessor or postprocessor. The analytical system also has a code for generating the input data for the next pass from the FEM analytical results of the current pass. This feature allows the analysis of multiple-pass rolling as well.

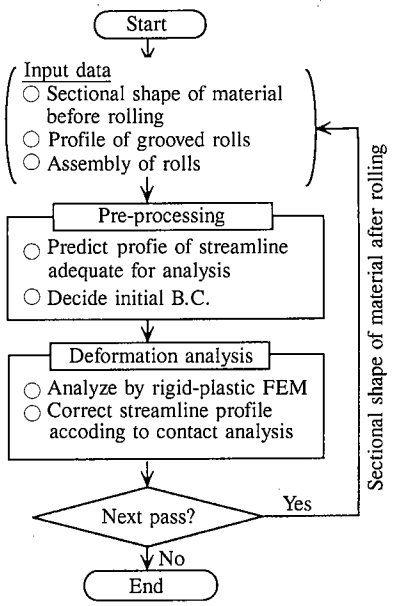

Fig. 1 Flow of analysis

The methods for correcting the streamline profile and predicting the initial streamline profile, two characteristics of the analytical system, are described below.

2.2 Method for correcting streamline profile

To determine the boundary conditions required for analyzing the velocity field, it is necessary to predict the surface profile of the material. In steady-state analysis, the predicted material surface profile must eventually agree with the streamline profile computed by integrating the obtained velocity field. Since the two do not always agree, however, it then becomes necessary to correct the discrepancy between the two and hence the boundary conditions. The accuracy and convergence of this analysis greatly changed with the methods employed for correcting the streamline profile and boundary conditions.

The methods for correcting the streamline profile and boundary conditions in the analytical system are shown in **Fig. 2**[9]. The streamline profile is corrected in two stages. The first stage involves the convergence computation, which is performed to determine whether or not each material surface node is in contact with the roll. The following operations are repeated until the boundary conditions converege:

(1) Integrate the nodal velocity vectors obtained under the predict boundary conditions, obtain the streamline profile of the material, and compare it with the roll surface profile.

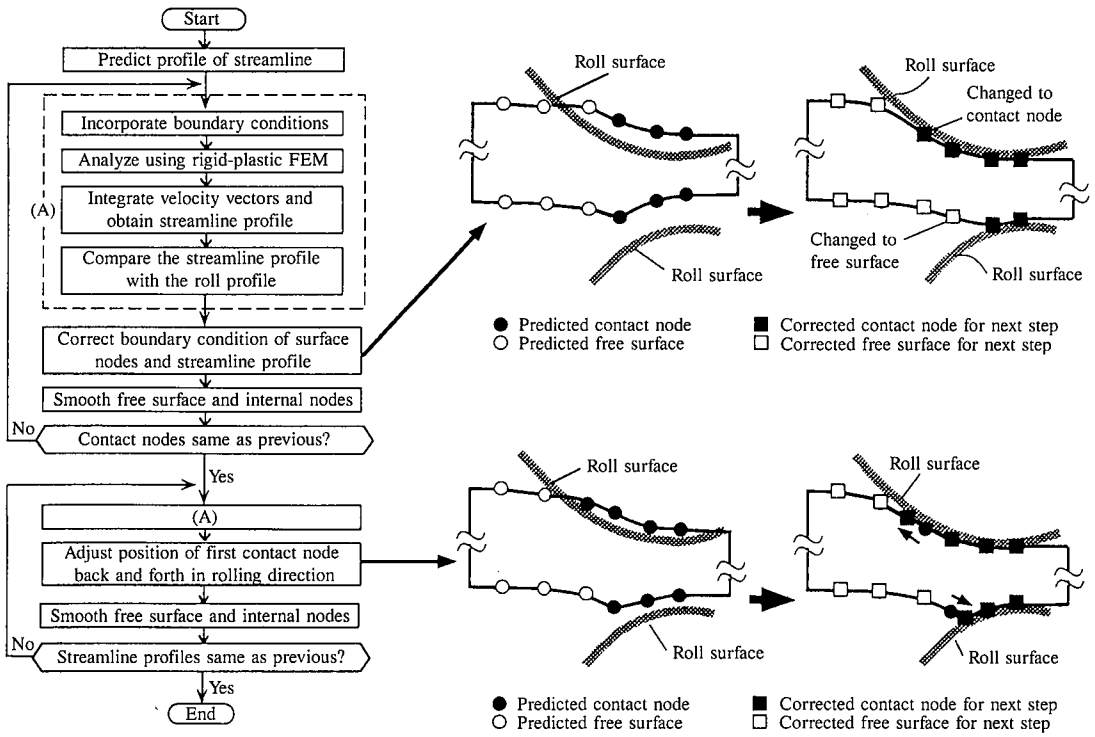

Fig. 2 Methods for correcting streamline profile and boundary conditions

(2) If a node assumed to be not in contact with the roll is actually positioned inside the roll, correct the boundary conditions to bring the node into contact with the roll.
(3) If a node assumed to be in contact with the roll is actually positioned outside the roll, change the boundary conditions for the first node so that it is in contact with the roll on the streamline. This will move the first node out of contact with the roll.
(4) Move the nodes positioned inside the roll onto the roll surface.
(5) In response to the movement of the nodes in contact with the roll, move the nodes positioned inside the material and on the free surface of the material so that the streamline profile can be smoothed.

In the second stage, the position of the material surface nodes in the rolling direction is adjusted to strictly determine the roll-material contact region. Like in the first stage, the velocity field is integrated, and the streamline profile is obtained and compared with the roll profile. If the streamline penetrates the roll, the position of the node that first contacts the roll is moved upstream. If a node predicted to be in contact with the roll is actually positioned outside the roll, the first contact position is moved downstream. These operations are repeated until the contact region converges. This method can accurately locate the contact region, even when the area near the roll-material first contact position cannot be divided into fine elements.

2.3 Method for predicting initial streamlines of material

Unless the appropriate streamline profile and boundary conditions are predicted at the beginning of the analysis, the accuracy and convergence of computation may deteriorate, and a solution may not be obtained even with the use of the method for correcting the boundary conditions as described in the previous section.

Initial streamlines for the steady-state analysis of rolling are generally determined according to the geometrical arrangement of the material and rolls. If only the top or bottom surface of the material contacts the roll as shown in **Fig. 3**, the material is sheared, and is also deformed where it does not come into contact with the roll. As described below (see **Fig. 4**), this analytical system takes this shear deformation into account when determining the initial streamline profile :

(1) Extend the entry cross-sectional profile of the material in the rolling direction, and compare it with the roll profile at each dividing point in the rolling direction.
(2) Move the material portions that penetrate the roll to the roll surface.
(3) Move the opposite surface of the material in response to the movement in step (2) above.
(4) Again compare the material profile with the roll profile, and move the material portions that penetrate the roll to the roll surface.

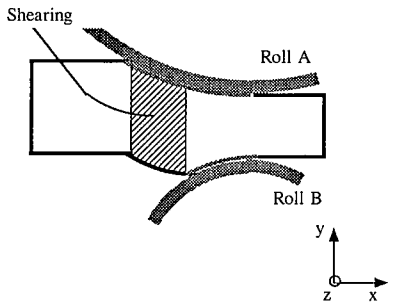

Fig. 3 Deformation of material by shear

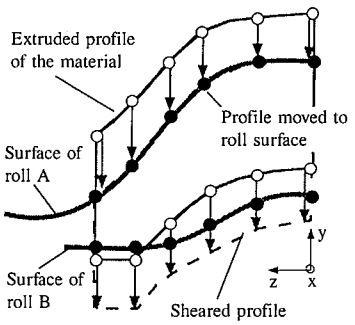

Fig. 4 Method for predicting initial streamline profile

3. Analysis of Long Steel Product Rolling

3.1 Analysis of hollow bloom rolling

Reduction of a bloom containing a liquid core at the end of continuous casting is known to reduce center segregation and center porosity[11]. This reduction also causes internal cracks in the liquid-core bloom. These phenomena are believed to be related to the flow of the liquid phase resulting from the deformation of the solidifying shell and to the stress that developed in the inside surface of the solidifying shell. To date, the rolling of material containing the liquid phase has been analyzed with respect to bloom reduction in the continuous casting process[12], but this type of analysis has not been conducted under such conditions that bloom reduction is heavy enough to weld shut the solidifying shell. Discussed here are the characteristics of liquid-core bloom rolling under a heavy bloom reduction as investigated by using the analytical system.

3.1.1 Analytical method and conditions

A hollow bloom without a liquid phase was analyzed by considering that the effect of the liquid phase on the deformation of the solidifying shell is small when the reduction is heavy enough to weld shut the solidifying shell. The analysis model is illustrated in **Fig. 5**. Given the symmetry of the hollow bloom, its quarter section was analyzed. Besides the rolling mill rolls, a flat tool causing a friction coefficient of 0 was assume to be present on the symmetric plane. When a hollow surface node reaches the symmetric plane, it is constrained by the flat tool. Since the velocity component in the reduction direction consequently becomes zero, the welding shut of the top and bottom surfaces of the hollow part can be thus simulated.

To verify the accuracy of the analytical model, the analytical results were compared with the results of plasticine experiments, and the effect of roll groove geometry on the deformation characteristics of the hollow bloom was studied. The analytical conditions are given in **Tables 1** and **2**. The roll groove shapes studied are shown in **Fig. 6**. The midwidth profile (arc or flat) and the width constriction were changed.

3.1.2 Analytical results

Fig. 7 shows the analytically and experimentally determined changes during rolling in the cross-sectional profile of a hollow bloom with an initial hole diameter of 35 mm. The hole initially changes from a circle to an ellipse in shape, and then begins to be welded shut from the sides. Under this condition, the hole is

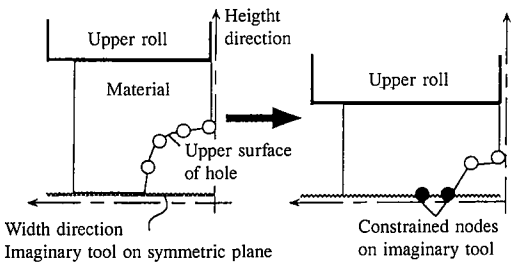

Fig. 5 Analytical model for hollow bloom rolling

Table. 1 Analytical conditions for hollow bloom rolling (comparison with experimental conditions)

Initial dimension of bloom (mm)	110×110
Initial diameter of hole (mm)	15,25,35
Roll diameter (mm)	350
Caliber geometry	Flat
Reduction in height (%)	40
Peripheral speed of roll ($m \cdot min^{-1}$)	1.0
Coefficient of friction	0.3(lubrication of talc)
Yield stress (MPa)	$\sigma = 0.182\,\varepsilon^{0.11}$

Table. 2 Analytical conditions for hollow bloom rolling (effect of roll groove geometry)

Initial dimension of bloom (mm)	220×220
Initial diameter of hole (mm)	30,50,70
Roll diameter (mm)	700
Reduction in height (%)	40
Peripheral speed of roll at width center ($m \cdot min^{-1}$)	2.0
Coefficient of friction	0.3
Yield stress (MPa)	$\sigma = 72\,\varepsilon^{0.21}\,\dot{\varepsilon}^{0.13}$

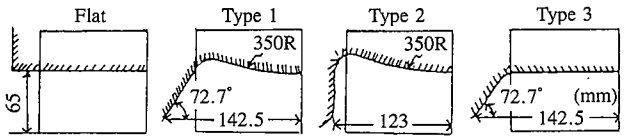

Type	Flat	1	2	3
Profile of width center	Flat	Arc	Arc	Flat
Constriction	None	Weak	Firm	Weak

Fig. 6 Roll groove geometries

completely closed at the exit side of the roll bite. The calculated and measured changes in the hole height during rolling are shown in **Fig. 8**. For the same rolling direction position, the greater the initial hole diameter, the smaller the hole height becomes. Under each condition, the analytical results agree closely with the experimental results.

The effect of roll groove geometry on the change in hole area during rolling is shown in **Fig. 9.** In the range analyzed here, hole area changes little with the roll groove geometry.

Fig. 10 shows the effect of roll groove geometry on the longitudinal stress produced at the midwidth of the hole surface during rolling. The stress is made nondimensional by the yield stress. The longitudinal stress reaches its maximam at the center of the roll bite, and the stress after the closure of the hole becomes compressive. The effect of roll groove geometry on this characteristic is small.

Fig. 11 shows the effect of roll groove geometry on the

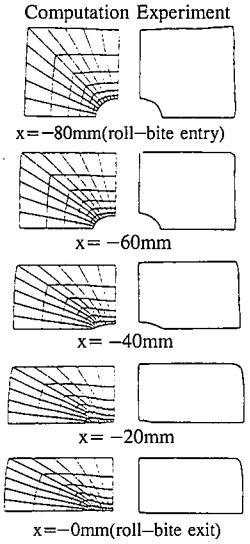

Fig. 7 Change in cross-sectional profile of material during rolling (initial hole diameter of 35 mm)

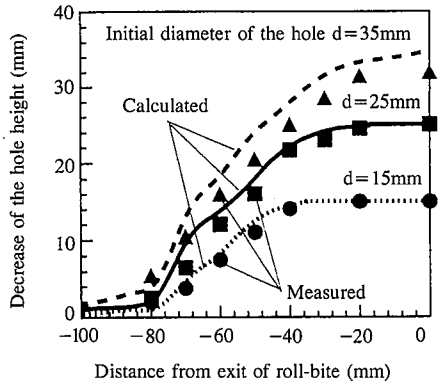

Fig. 8 Change in hole height during rolling

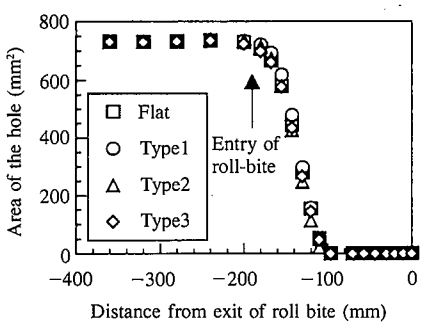

Fig. 9 Change in hole area during rolling (initial hole diameter of 30 mm)

transverse stress developed at the midwidth of the hole surface during rolling. The transverse stress reaches its maximum at the entry side of the roll bite and becomes compressive after the welding shut of the hole. When the width constraint is strong or the roll groove is flat at the center, the transverse compressive stress developed after the welding shut of the hole increases.

Fig. 12 shows the effects of the initial hole diameter and roll groove geometry on the maximum values of the longitudinal and transverse stresses. The maximum value of the longitudinal stress is affected little by the initial hole diameter and roll groove geom-

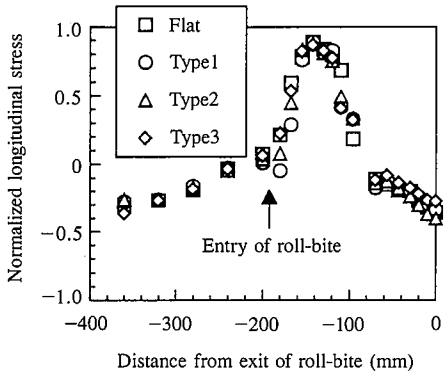

Fig. 10 Effect of roll groove geometry on longitudinal stress developed at midwidth of hole (initial hole diameter of 30 mm)

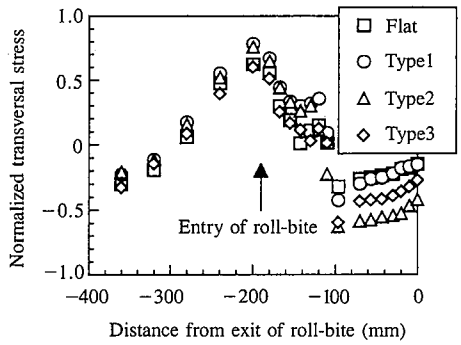

Fig. 11 Effect of roll groove geometry on transverse stress developed at midwidth of hole (initial hole diameter of 30 mm)

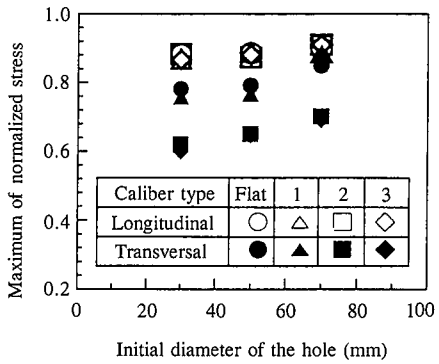

Fig. 12 Effects of initial hole diameter and roll groove geometry on maximum values of longitudinal and transverse stresses

etry, and is large at about 90% of the yield stress. These conditions increase the possibility of longitudinal cracking. The maximum value of the transverse stress rises with increasing initial hole diameter and by using a roll groove with an arc at the midwidth. When a bloom with an initial hole diameter of 70 mm is rolled in a roll groove with an arc at the midwidth, the maximum transverse and longitudinal stresses are approximately equal. From this result, it is expected that the direction of cracking will change with rolling conditions.

3.2 Rolling of angles

3.2.1 Analytical conditions

In the rolling of a material asymmetrical in the vertical direction, changing the height of the passline alters the material profile

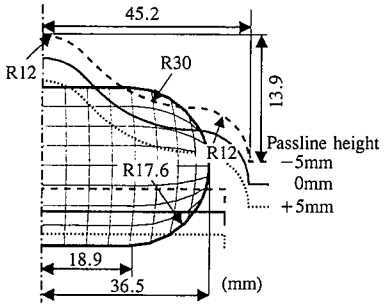

Fig. 13 Material shape before rolling and roll groove geometry

Table. 3 Analytical conditions for angle rolling

Roll diameter at width center(mm)	120(upper) 130(lower)
Peripheral speed of rolls at width center(m·min^{-1})	4.0
Passline height(mm)	−5,0,5
Coefficient of friction	0.3
Yield stress(MPa)	$\sigma = 82\,\varepsilon^{0.21}\,\dot{\varepsilon}^{0.13}$

after rolling. This passline effect was studied by taking the rolling of angles as an example. The analyzed material and roll groove profiles are shown in **Fig. 13**, and the analytical conditions are given in **Table 3**. The height of the passline at which the material contacts the top and bottom rolls at the same time is put at zero, and the height of the pass line at which the material first contacts the top roll is denoted by a positive value.

3.2.2 Analytical results

The contact area predicted at the beginning of the analytical process and the rolling pressure distribution after convergence are shown in **Fig. 14**. When the passline height is set at −5 mm and 0 mm, the rolling pressure distributions are similar. When the passline height is set at +5 mm, the rolling pressure at the transverse edge of the bottom roll increases toward the entry side of the roll bite. When the passline height is set at −5 mm and 0 mm, the material contacts the bottom roll at approximately the same time. When the passline is +5 mm, the reduction of the top roll moves down the transverse edges of the material and causes material contact to occur first at the transverse edges. Comparison of the contact area predicted in the initial phase of the analysis with the contact area after the convergence shows that the two approximately agree in profile, although predeformation changes the first contact position. This verifies the validity of the method employed by the analytical system for determining the initial streamlines.

The effect of the passline height on the material profile after rolling is shown in **Fig. 15**. The head fill and spread increase with decreasing passline height and greater contact length with the bottom roll. The effect of the passline height on the equivalent strain distribution is shown in **Fig. 16**. The equivalent strain maximizes in the surface where the material contacts the top roll, and the effect of the passline height is small in this area. The equivalent strain at the transverse edges in the surface where the material contacts the bottom roll increases as the passline height becomes greater.

3.3 Web width increase rolling of H shapes

One technology for manufacturing H shapes with fixed outer dimensions involves increasing the web width by using a skew

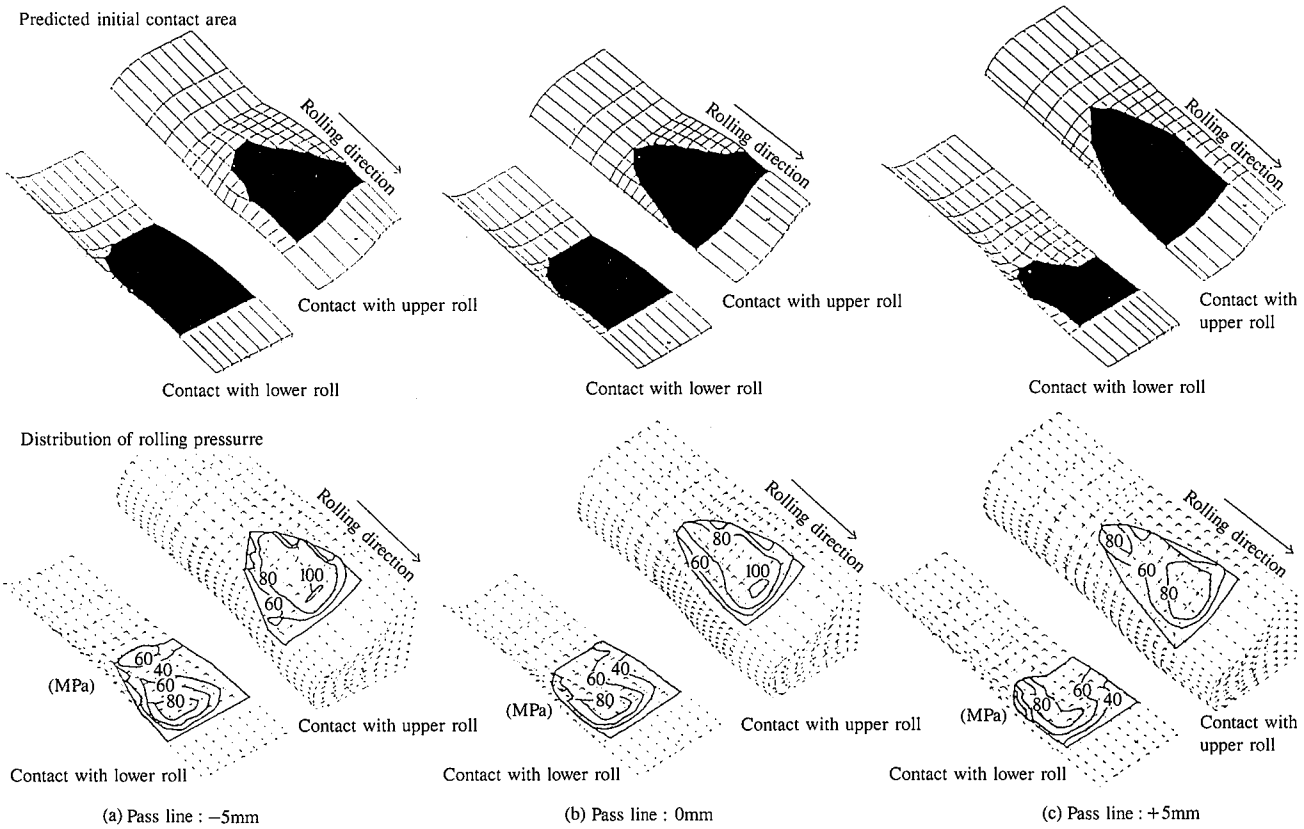

Fig. 14 Initial contact area and rolling pressure distribution

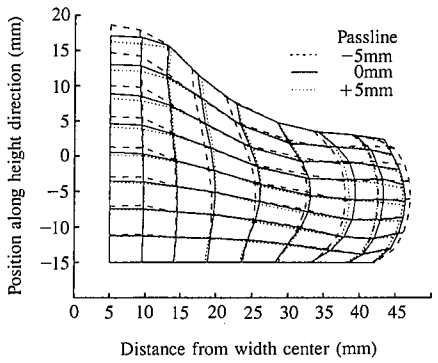

Fig. 15 Effect of passline height on material shape after rolling

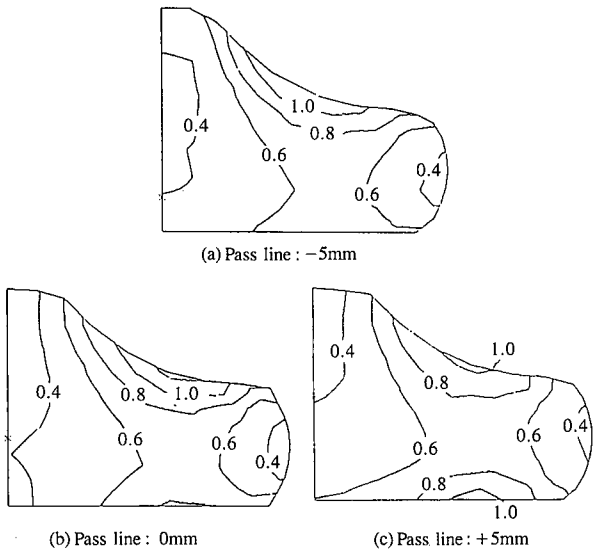

Fig. 16 Effect of passline height on equivalent strain distribution

roll mill[13]. The method of increasing the web width of H shapes with the skew roll mill is illustrated in **Fig. 17**. The four rolls are arranged with the cross angle α with respect to the rolling direction and the inclination angle β with respect to the vertical direction. While expanding the flanges with their sides, these rolls reduce web end thickness, and increase the web width.

3.3.1 Analytical conditions

The analytical conditions are listed in **Table 4**. The cross angle was set at 0, 5 and 10 degrees, and then investigated. In web width increase rolling with the skew roll mill, the web width increases with expanding cross angle if distance between rolls is constant. In this analysis, the roll gap was adjusted to ensure the same web width increase under all conditions.

3.3.2 Analytical results

The effect of the cross angle on the cross-sectional shape after rolling is shown in **Fig. 18**. As the cross angle increases, the flange tilt angle and the flange width rise. The larger flange width and the greater cross angle may be explained as follows. In skew roll rolling, there are regions before and after the roll bite where the web width expands because of pressure from the inside

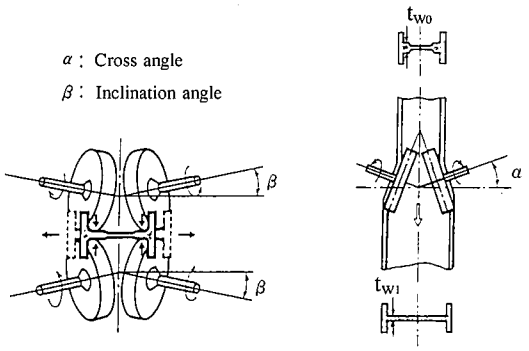

Fig. 17 Web width increase rolling with skew roll mill

Table. 4 Analytical conditions for web width increase rolling of H shapes

Initial dimension of H-beam/H×B×t_w/t_f(mm)	570×200×9.8/14.7
Roll diameter(mm)	900
Cross angle(degree)	0,5,10
Inclination angle(degree)	5
Web height expansion(mm)	30
Coefficient of friction	0.3
Yield stress(MPa)	$\sigma = 150\,\varepsilon^{0.21}\,\dot{\varepsilon}^{0.13}$

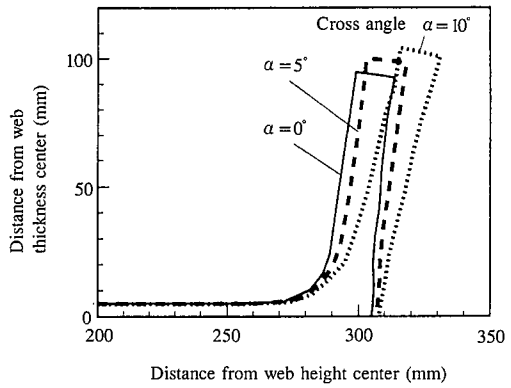

Fig. 18 Effect of cross angle on material shape after rolling

surface of each flange. In the region before the roll bite, the inside surface of the flange is forced down by the rolls,thereby decreasing the flange width. In the region after the roll bite, the inside surface of the flange is forced up by the rolls,thereby increasing the flange width. The regions before and after the roll bite alter depending on the cross angle. Raising the cross angle decreases the width increase in the region before the roll bite and reduces the area forced down by the rolls. It also increases the width expansion in the region after the roll bite and increases the area forced up by the rolls. The net result is increased flange width.

The effect of the cross angle on longitudinal stress distribution at the midthickness of the H shape is shown in **Fig. 19**. Longitudinal stress greatly changes depending on the cross angle. Particularly, increasing the cross angle reduces the compressive stress at either end of the web. This is because the increase in the cross angle facilitates the flow of metal in the web width direction and reduces the difference in elongation between the web width center and ends.

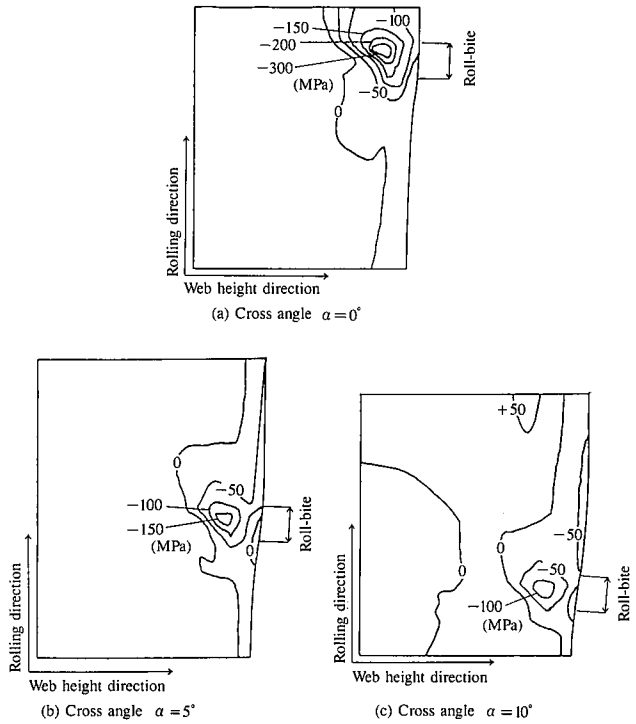

Fig. 19 Effect of cross angle on longitudinal stress distribution

4. Conclusions

A system was developed for analyzing the rolling of long steel products using the rigid-plastic finite element method. This system can analyze rolling with any material shape, roll groove geometry and roll arrangement. It is used for research and development on new rolling processes and for improving the operating conditions of conventional rolling processes.

References

1) Bertrand, C. et al.: NUMIFORM 86. 1986, p. 207-212
2) Mori, K. et al.: NUMIFORM 89. 1989, p. 337-343
3) Nikaido, H. et al.: Journal of Japan Society for Technology of Plasticity. 31 (350), 378 (1990)
4) Toyoshima, S. et al.: Journal of Japan Society for Technology of Plasticity. 31 (350), 398 (1990)
5) Yanagimoto, J. et al.: Journal of Japan Society for Technology of Plasticity. 34 (384), 75 (1993)
6) Yanagimoto, J. et al.: Journal of Japan Society for Technology of Plasticity. 36 (408), 41 (1995)
7) Mori, K. et al.: Journal of Japan Society for Technology of Plasticity. 34 (384), 100 (1993)
8) Yamada, K. et al.: NUMIFORM 89. 1989, p. 375-308
9) Ida, M. et al.: Proceedings of 1990 Japanese Spring Conference for Technology of Plasticity. 1990, p. 61-64
10) Mori, K. et al.: Transactions of Japan Society of Mechanical Engineers, Series A. 45 (396), 965 (1979)
11) Takehara, E. et al.: Tetsu-to-Hagané. 60 (7), 138 (1974)
12) Pawelski, K. et al.: NUMIFORM 92. 1992, p. 743-747
13) Ikuta, K. et al.: Proceedings of 40th Japanese Joint Conference for Technology of Plasticity. 1989, p. 389-393